

AD-A045 173

NAVAL POSTGRADUATE SCHOOL MONTEREY CALIF

SIMULATION OF A CONTROLLABLE REVERSIBLE PITCH (C.R.P.) PROPELLER--ETC(U)

F/0 13/10

JUN 77 M KANAZAWA

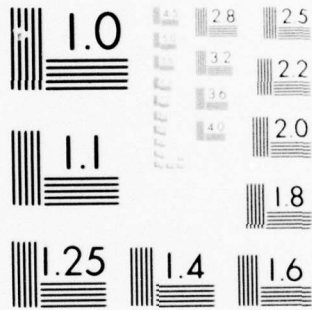
UNCLASSIFIED

NL

| OF |  
AD-A045173



END  
DATE  
FILMED  
11 - 77  
DDC



MICROCOPY RESOLUTION TEST CHART  
NATIONAL BUREAU OF STANDARDS-1963-A

*[Handwritten signature]* 2

AD A 045173

# NAVAL POSTGRADUATE SCHOOL

Monterey, California



# THESIS

DDC  
RECEIVED  
OCT 14 1977  
D

SIMULATION OF A CONTROLLABLE  
REVERSIBLE PITCH (C.R.P.) PROPELLER SYSTEM  
by  
Masaaki Kanazawa  
June 1977  
Thesis Advisor: T. M. Houlihan

AD No. \_\_\_\_\_  
DDC FILE COPY

Approved for public release; distribution unlimited.

SECURITY CLASSIFICATION OF THIS PAGE (When Data Entered)

REPORT DOCUMENTATION PAGE		READ INSTRUCTIONS BEFORE COMPLETING FORM
1. REPORT NUMBER	2. GOVT ACCESSION NO.	3. RECIPIENT'S CATALOG NUMBER
6 4. TITLE (and Subtitle) Simulation of a Controllable Reversible Pitch (C.R.P.) Propeller System,		9 5. TYPE OF REPORT & PERIOD COVERED Master's Thesis June 1977
10 7. AUTHOR(s) Masaaki Kanazawa		6. PERFORMING ORG. REPORT NUMBER
9. PERFORMING ORGANIZATION NAME AND ADDRESS Naval Postgraduate School Monterey, California 93940		8. CONTRACT OR GRANT NUMBER(s)
11. CONTROLLING OFFICE NAME AND ADDRESS Naval Postgraduate School Monterey, California 93940		10. PROGRAM ELEMENT, PROJECT, TASK AREA & WORK UNIT NUMBERS
14. MONITORING AGENCY NAME & ADDRESS (if different from Controlling Office) Naval Postgraduate School Monterey, California 93940		12. REPORT DATE June 1977
12. 44p.		13. NUMBER OF PAGES 44
15. SECURITY CLASS. (of this report) Unclassified		15a. DECLASSIFICATION/DOWNGRADING SCHEDULE
16. DISTRIBUTION STATEMENT (of this Report) Approved for public release; distribution unlimited.		
17. DISTRIBUTION STATEMENT (of the abstract entered in Block 20, if different from Report)		
18. SUPPLEMENTARY NOTES		
19. KEY WORDS (Continue on reverse side if necessary and identify by block number)		
20. ABSTRACT (Continue on reverse side if necessary and identify by block number) A computer model was developed to simulate a C.R.P. propeller system. A set of simultaneous differential equations was solved using CSMP III-the IBM simulation language. The computer model was verified against manufacturer's data. Power piston displacement, → cont on p 2		

DD FORM 1473  
1 JAN 73  
(Page 1)

EDITION OF 1 NOV 68 IS OBSOLETE  
S/N 0102-014-6601

SECURITY CLASSIFICATION OF THIS PAGE (When Data Entered)

251 450 1

LB

*Cont for P I*

↳ power piston velocity and chamber pressure were determined for a nominal supply pressure of 600 PSI and various loadings. Overall, the system model and data should prove useful for investigations of design variations.

✱

ACCESSION for		
NTIS	White Section	<input checked="" type="checkbox"/>
DOC	Buff Section	<input type="checkbox"/>
UNANNOUNCED		<input type="checkbox"/>
JUSTIFICATION.....		
BY.....		
DISTRIBUTION/AVAILABILITY CODES		
Dist.	AVAIL. and/or	SPECIAL
A		

Approved for public release; distribution unlimited.

Simulation of a Controllable  
Reversible Pitch (C.R.P.) Propeller System

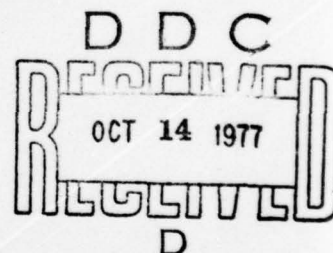
by

Masaaki Kanazawa  
Lieutenant, Japan Maritime Self Defence Force  
B.S., Tohoku Gakuin University, 1967

Submitted in partial fulfillment of the  
requirements for the degree of

MASTER OF SCIENCE IN MECHANICAL ENGINEERING

from the  
NAVAL POSTGRADUATE SCHOOL  
June 1977



Author

Masaaki Kanazawa

Approved by:

Thomas H. Hurlburt  
Thesis Advisor

Robert A. Fossum  
Second Reader

Allen E. Fuhs  
Chairman, Department of Mechanical Engineering

Robert A. Fossum  
Dean of Science and Engineering

#### ABSTRACT

A computer model was developed to simulate a C.R.P. propeller system. A set of simultaneous differential equations was solved using CSMP III-the IBM simulation language. The computer model was verified against manufacturer's data. Power piston displacement, power piston velocity and chamber pressure were determined for a nominal supply pressure of 600 PSI and various loadings. Overall, the system model and data should prove useful for investigations of design variations.

TABLE OF CONTENTS

I.	INTRODUCTION - - - - -	11
II.	BACKGROUND - - - - -	12
	A. BASIC CONTROL CONCEPTS - - - - -	12
	B. ANALYTICAL APPROACH - - - - -	15
III.	CONSTITUENT RELATIONSHIPS - - - - -	18
	A. INPUT SERVOVALVE AND PISTON - - - - -	18
	B. POWER PISTON - - - - -	19
	C. OVERALL SYSTEM - - - - -	20
IV.	SYSTEM STATE EQUATIONS - - - - -	23
V.	ANALYSIS OF SYSTEM PERFORMANCE - - - - -	25
	A. PROCEDURE - - - - -	25
	1. Inputs - - - - -	25
	2. Outputs - - - - -	25
	B. COMPUTER SIMULATION RESULT - - - - -	27
VI.	CONCLUSIONS - - - - -	34
	APPENDIX A: SYSTEM SIGNAL FLOW GRAPH - - - - -	35
	APPENDIX B: SYSTEM RESPONSE - - - - -	36
	APPENDIX C: COMPUTER PROGRAM - - - - -	38
	APPENDIX D: FLUID LINE RESPONSE - - - - -	40
	LIST OF REFERENCES - - - - -	43
	INITIAL DISTRIBUTION LIST - - - - -	44



LIST OF TABLES

I. List of Constants - - - - - 22

LIST OF FIGURES

1.	Block Diagram of a Closed-Loop System - - - - -	12
2.	Valve Controlled Piston - - - - -	13
3.	Position Control System Response (Open-Loop) - - - - -	14
4.	Geometry of a Basic C.R.P. System - - - - -	17
5.	System Equations (Matrix Notation) - - - - -	24
6.	Scheduling of Control Parameters - - - - -	26
7.	Displacement Response of Power Piston - - - - -	28
8.	Steady State Velocity Response of Power Piston - - - - -	29
9.	Pressure Response of Power Piston - - - - -	30
10.	Bulk Modulus Effects on Response - - - - -	31
11.	Initial Velocity Response of Power Piston - - - - -	33
12.	System Signal Flow Graph - - - - -	35
13.	Signal Flow Graph of Input Parts - - - - -	36
14.	Signal Flow Graph of Output Parts - - - - -	37
15.	Computer Program Output - - - - -	39
16.	Circular Type of Line Response Determinations - - - - -	40
17.	Annular Type of Line Response Determinations - - - - -	41
18.	Double Annular Type of Line Response Determinations - - - - -	42

## NOMENCLATURE

A	cross-section area
B	load damping coefficient
C	leakage coefficient
F	force
K	load spring constant
$K_c$	valve pressure coefficient
$K_q$	valve flow gain
$K_f$	flow force spring rate
M	mass
$P_m$	load pressure on power piston
$P_{la}$	load pressure on input piston
$P_s$	supply pressure on power piston
$P_{sa}$	supply pressure on input servovalve
Q	flow rate
t	time
V	volume
w	valve area gradient
X	input piston displacement
$X_{va}$	valve displacement
Y	power piston displacement
$\beta_e$	effective bulk modulus
$\zeta$	damping factor
$\omega_h$	natural frequency

## SUBSCRIPTS

a        refers to input piston  
l        refers to load  
m        refers to power piston  
p        refers to piston  
s        refers to supply pressure  
v        refers to valve

#### ACKNOWLEDGEMENTS

I acknowledge my indebtedness to Professor Thomas M. Houlihan for his helpful advice and suggestions. Appreciation is also expressed to Professor Robert D. Strum for his fine instruction in control theory.

I would also like to offer my special thanks to my wife, Mitsue, for being understanding and patient during this time.

## I. INTRODUCTION

During recent years, naval applications of gas turbine engine systems have become more prominent. At first, the gas turbine engine was developed as an aircraft power source. Presently, it is entering service as a marine power source. Gas turbine engine systems have several advantages compared to other power systems. The main advantages are its relative compactness and the fact that the rotating output of the turbine is usually what is wanted to turn a wheel, propeller, generator, or pump. Unfortunately, compared to other systems, there is a problem of matching the characteristics of the load and the engine. In this respect, controllable reversible pitch (C.R.P.) propellers are useful.

Controllable pitch propellers, unlike fixed pitch propellers, have the ability to reverse thrust through a reversal of pitch rather than a reversal of rotation. The controllable pitch propeller is much more complex than a solid propeller and contains many more parts [1]. However, the operation of a C.R.P. system provides a greater degree of flexibility in the maneuvering and docking of ships.

Since there is an increasing interest in the application of controllable reversible pitch propellers to naval vessels, the objectives of this study were as follows:

1. to determine an overall analytical model of an operational C.R.P. system;
2. to check the system response for design variations.

## II. BACKGROUND

### A. BASIC CONTROL CONCEPTS

In a control system in which the output appears as mechanical energy, the quantity to be controlled can be either load, torque, position, or velocity and can be controlled under either open- or closed-loop conditions. In an open-loop system [2], the input is fed to the controller which then operates on the output. The input, being an independent variable, is incapable of correcting any errors between the desired and actual output.

The accuracy of an open-loop system is, therefore, greatly affected by external disturbances and variations of system parameters. In a closed-loop system [2], the output is fed back and compared with the desired value. The error between the desired and actual output is fed into the control elements which in turn operate on the output, tending to reduce or null the error. This is the concept of negative feedback. A block diagram of a closed-loop system is shown in Figure 1.

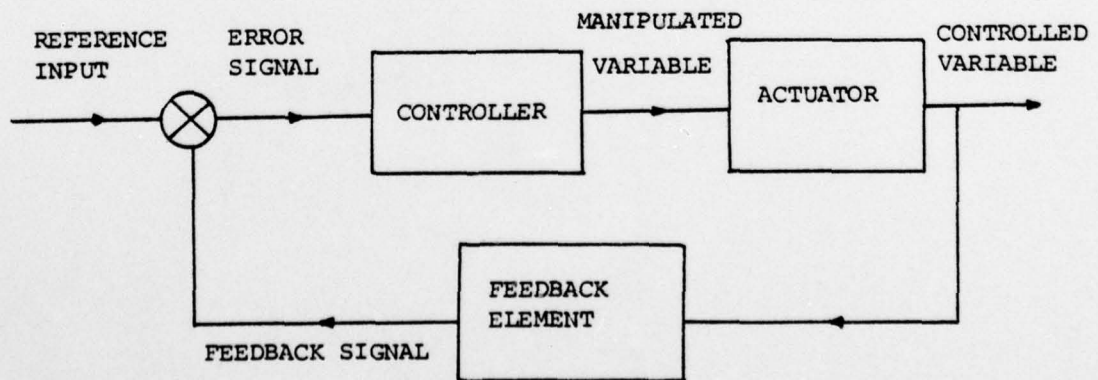


Figure 1. Block Diagram of a Closed-Loop System.

In a position control system in which the manipulated variables are pressure and flow, the hydraulic quantities are converted into a displacement by action on the piston rod or output shaft. The two properties of flow which can be manipulated are its direction and magnitude. Directional control of flow is used for simple position control systems under both open- and closed-loop conditions [3].

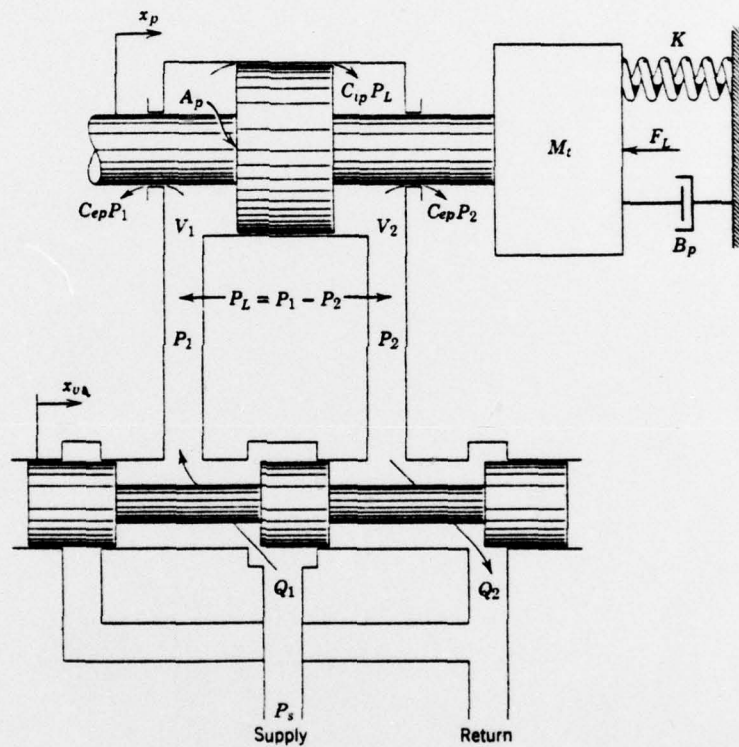


Figure 2. Valve Controlled Piston.

Directional control valves that could be used here are of the three- or four-way type. A schematic arrangement of a four-way valve controlling a symmetrical piston is shown in Figure 2.

When the control valve as shown is in the neutral position, the piston is hydraulically locked. A displacement of the valve spool in either direction causes the piston to move in the opposite sense.



An idealized graph of a position control system which is operated under open-loop conditions, by a directional control valve is shown in Figure 3.

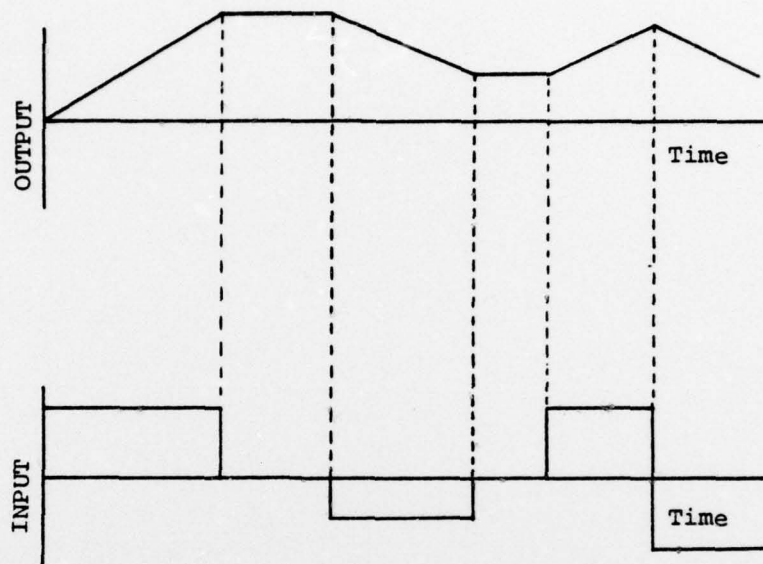


Figure 3. Position Control System Response (Open-Loop).

When the valve is displaced from its neutral position, the actuator moves at constant velocity in the required direction until the valve is returned to neutral. An open-loop system of this type is only suitable for simple applications which do not require accurate piston control.

Closed-loop position control systems employ controllers having non-continuous or "on-off" characteristics. When the actuating signal reaches a threshold value, the directional control valve becomes operative and causes the actuator to move at constant velocity in the chosen direction. It continues to move until the error signal falls below the threshold value. This causes the valve to return to its closed position and stop the motion of the piston.

The most widely used type of control for hydraulic positioning servo systems is the control flow type, where both flow direction and magnitude are manipulated. The two methods of achieving flow control are:

1. controlling the displacement of a variable delivery pump;
2. throttling fluid through the variable orifices of a control valve.

The two basic differences between pump operated and valve operated servo systems can be described as follows:

1. In pump operated servos, working pressure is variable, depending on the external loading, while valve controlled servos operate at constant system pressure.
2. In valve controlled servos, power sources are outside the loop.

In this study, a valve controlled servo system was studied.

#### B. ANALYTICAL APPROACH

This analytical investigation was directed toward predicting various C.R.P. system pressures and motions. An analytical model was developed using first-order differential equations. The mathematical model, which was programmed on a digital computer, predicted the position and velocity of the power piston and the pressure at various points in the system as a function of time. Further analysis was performed using the model to obtain preliminary predictions of system performance under a variety of external loadings.

To understand the derivation in the following sections, Figure 4 indicates the geometry of a basic controllable reversible pitch (C.R.P.) propeller system. Beginning with the input side, a force balance on the

input servovalve yielded an equation for the load pressure on the input piston in terms of the valve motion. The input piston was moved by load pressure,  $P_{\lambda a}$ . The valve rod control assembly was moved by the force exerted on the input piston. This caused the primary supply pressure,  $P_s$ , to pass through the hub valve into the power piston and move the propeller crank-slot pin. This power piston control system, as such, is similar in operation to a vehicular power-assisted steering mechanism.

To facilitate the digital simulation it was assumed that the input valve spool displacement,  $X_{va}$ , and the arbitrary load,  $F_\lambda$ , were step inputs. In the process of solution, the system state equations were solved using CSMP III, the IBM simulation language.

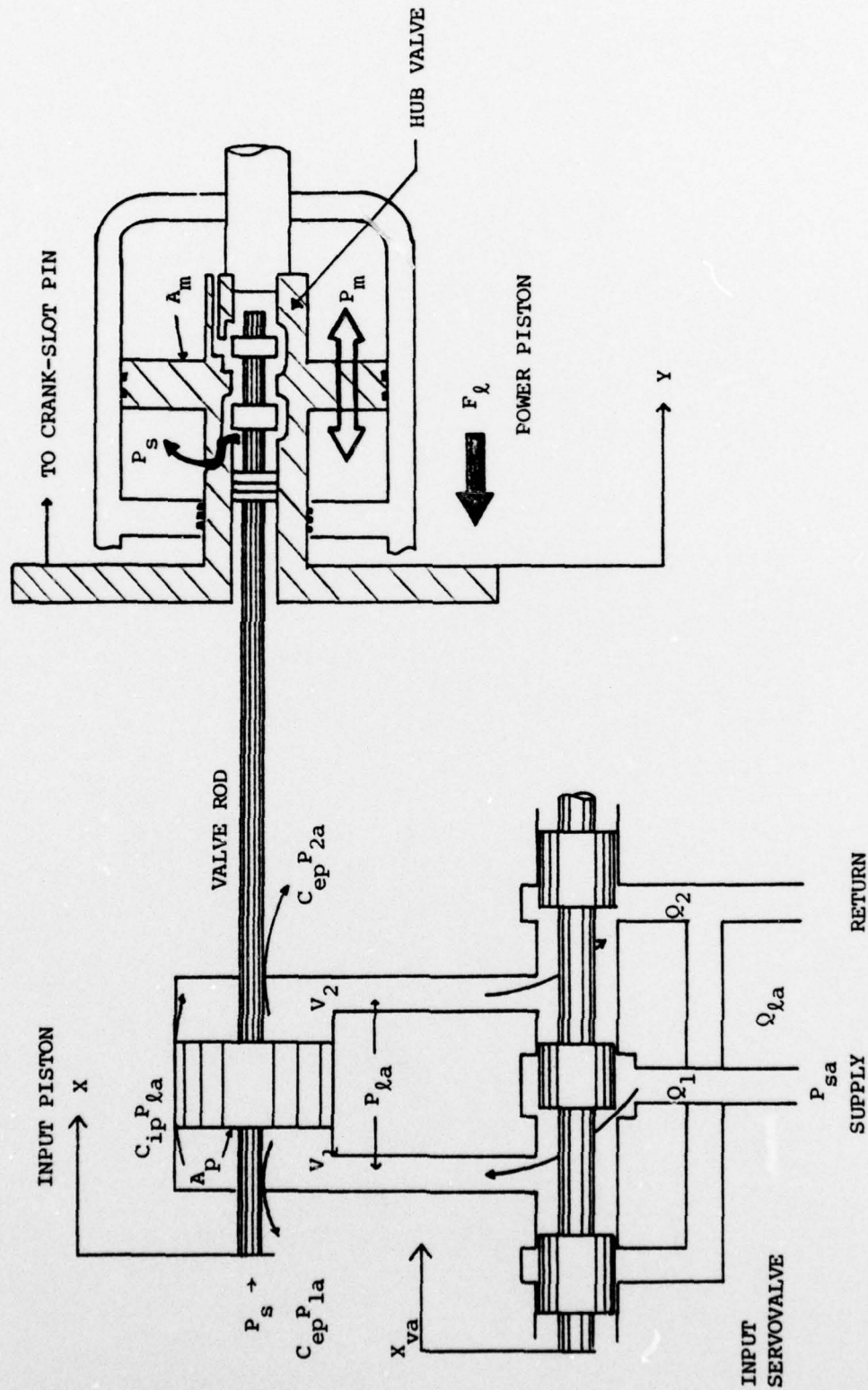


Figure 4. Geometry of a Basic C.R.P. System.

### III. CONSTITUENT RELATIONSHIPS

It was a difficult problem to identify the dynamic characteristics of the controllable pitch propeller system because of its essentially nonlinear behavior. Identification was partially achieved by assuming that these responses were linear and then applying parameter estimation for linear systems.

#### A. INPUT SERVOVALVE AND PISTON

The combination of a servovalve and a piston is a common hydraulic power element [3]. In analyzing this simple system, three basic relationships surface. The first concerns the valve, the second concerns the piston dynamics and the third concerns the flow of hydraulic fluid between the elements.

Regarding the valve, the basic equation that pertains is

$$Q_{la} = K_{qa} X_{va} - K_{ca} P_{la} \quad (1)$$

where

$$K_{qa} = 70 w_a \sqrt{P_{sa}}$$
$$K_{ca} = \frac{Q_{la}}{P_{sa}}$$

Regarding the piston, the basic equation governing valve dynamics is

$$\Sigma F_p = M_v \ddot{X} \quad (2)$$

The sum of the force acting on the piston is

$$\Sigma F_p = F_{pl} - F_{la} - K_{pa} X - B_{pa} \dot{X} \quad (3)$$

where

$$F_{pl} = A_p P_{la}$$

$$F_{la} = K_f (X - Y) = 0.86 w_m (P_s - P_m) (X - Y)$$

Combining equations (2) and (3) gives

$$A_p P_{la} = M_v \ddot{X} + B_{pa} \dot{X} + K_{pa} X + F_{la} \quad (4)$$

The flow relationship between the two elements is developed by applying the continuity equation to each of the piston chambers. In final form, this continuity relation becomes

$$Q_{la} = C_{tpla} P_{la} + A_p \dot{X} + \left( \frac{V_a}{4 \beta_e} \right) \dot{P}_{la} \quad (5)$$

where  $C_{tpla}$  is an overall leakage coefficient.

Equations (1), (4) and (5) are the basic equations of this subsystem.

#### B. POWER PISTON

From the characteristic equation of the critical center spool valve (hub valve), one can derive

$$Q_m = K_{qm} (X - Y) - K_{cm} P_m \quad (6)$$

$$\text{where } K_{qm} = 140 w_m \sqrt{P_s}$$

$$K_{cm} = \frac{Q_s}{P_s}$$

In a manner similar to the development of equation (5), the continuity expressions for the hub valve can be combined to yield

$$Q_m = C_{tp\ell m} P_m + A_m \dot{Y} + \left(\frac{V_m}{4\beta_e}\right) P_m \quad (7)$$

where  $C_{tp\ell m}$  is an overall leakage coefficient.

The final equation arises by applying Newton's second law to the power piston [4]. The resulting force equation is

$$A_{pm} P_m = M_{\ell} \ddot{Y} + B_{pm} (\dot{X} - \dot{Y}) + K_{pm} (X - Y) + F_{\ell} \quad (8)$$

Equations (6), (7) and (8) are the basic equations of the power piston system.

#### C. OVERALL SYSTEM

In analyzing the overall system, two modes of operation became apparent. First, if the system input was a forward valve displacement,  $X_{va}$ , the output was a power piston position and velocity. The second mode occurred during recovery from an external loading. For this mode, the input was an external load,  $F_{\ell}$ . At this point, it was necessary to simplify the governing equations. Usually, the loading on a valve controlled piston system is simpler than the most general in two respects [3]. First, significant spring loads are usually absent and hence  $K_{pa} = K_{pm} = 0$ . Second, damping loads are likewise negligible and then  $B_{pa} = B_{pm} = 0$ .

Thus, equation (8) reduced to

$$\ddot{Y} = \frac{1}{M_l} (A_m P_m - F_l) \quad (9)$$

A combination of equations (6) and (7) produced

$$\dot{P}_m = \frac{4 \beta e}{V_m} (-K_{cem} P_m - A_m \dot{Y} + K_{qm} X - K_{qm} Y) \quad (10)$$

Equation (4) was simplified to

$$\ddot{X} = \frac{1}{M_v} (-K_f X + K_f Y + A_p P_{la}) \quad (11)$$

Finally equations (1) and (5) yielded

$$\dot{P}_{la} = \frac{4 \beta e}{V_a} (-K_{cea} P_{la} - A_p \dot{X} + K_{qa} X_{va}) \quad (12)$$

Equations (9-12) were the governing equations for the C.R.P. system. The following is a listing of the constants used in the derivation of these governing equations and in the accompanying computer solution. The valves were derived from manufacturer's data [5].



TABLE I  
LIST OF CONSTANTS

$A_p$ (AA)	cross-sectional area of input piston	57.67 in
$A_m$ (AM)	cross-sectional area of power piston	1102.0 in
$K_{cm}$ (CEM)	flow gain of input servovalve	1.54 in <sup>3</sup> /sec/PSI
$K_{ca}$ (CEA)	flow gain of power piston	0.11 in <sup>3</sup> /sec/PSI
$V_a$ (VA)	total volume of input piston	749.71 in <sup>3</sup>
$V_m$ (VM)	total volume of power piston	14326.0 in <sup>3</sup>
$w_a$ (—)	valve gradient of input servovalve	1.571 in <sup>2</sup> /in
$w_m$ (W)	valve gradient of power piston	11.938 in <sup>2</sup> /in
$P_s$ (PS)	supply pressure (power piston)	400.0 PSI
$P_{sa}$ (PSA)	supply pressure (input servovalve)	600.0 PSI
$\beta_e$ (BE)	bulk modulus	100000.0 PSI
$M_l$ (XM)	total mass of power piston and propeller	69.8757 lb-sec <sup>2</sup> /in
$M_v$ (VM)	total mass of input piston and valve rod assembly	4.9 lb-sec <sup>2</sup> /in
$K_{qa}$ (QAK)	total flow pressure coefficient of input piston and servovalve	2057.08 in <sup>3</sup> /sec/in
$K_{qm}$ (QMK)	total flow pressure coefficient of power piston	33426.54 in <sup>3</sup> /sec/in

#### IV. SYSTEM STATE EQUATIONS

The system equations were first written in a state variable format [6]. Thus, in matrix notation, the system state equations became

$$\dot{X}(t) = A X(t) + B U(t)$$

Here  $X(t)$  was the matrix of system state variables and  $U(t)$  was the matrix of system input. From the overall system equations (9-12),  $Y(t)$ ,  $P_{\ell a}(t)$ ,  $X(t)$  and  $P_m(t)$  were chosen as the basic problem variables, and  $X_{va}$  and  $F_\ell$  became the input variables. Thus, the applicable state variables were

$$\begin{array}{llll} Y = X(1) & X = X(4) & P_m = X(3) & P_{\ell a} = X(6) \\ \dot{Y} = X(2) & \dot{X} = X(5) & \dot{P}_m = \dot{X}(3) & \dot{P}_{\ell a} = \dot{X}(6) \\ \ddot{Y} = \dot{X}(2) & \ddot{X} = \dot{X}(5) & & \end{array}$$

$$U_1 = X_{va} \quad U_2 = F_\ell$$

For example from equation (9) one can write

$$X(2) = \frac{A_m}{M_\ell} X(3) - \frac{1}{M_\ell} U_2 \quad (13)$$

In a similar way, the system equations were rewritten in matrix notation (Figure 5). The accompanying signal flow graph for the overall system equations is presented in Appendix A. The state equations were solved for various servovalve stroke values,  $X_{va}$ , and for various loading,  $F_\ell$ , using the IBM simulation language CSMP III as shown in the next section.

$$\begin{bmatrix} \dot{X}_1 \\ \dot{X}_2 \\ \dot{X}_3 \\ \dot{X}_4 \\ \dot{X}_5 \\ \dot{X}_6 \end{bmatrix} = \begin{bmatrix} 0 & 1 & 0 & 0 & 0 & 0 \\ 0 & 0 & \frac{A_{ml}}{M_l} & 0 & 0 & 0 \\ -\frac{4\beta_e K_{g-m}}{V_{mL}} & -\frac{4\beta_e A_{mL}}{V_{mL}} & -\frac{4\beta_e K_{cm}}{V_{mL}} & \frac{4\beta_e K_{gm}}{V_{mL}} & 0 & 0 \\ 0 & 0 & 0 & 1 & 0 & 0 \\ \frac{K_f}{M_v} & 0 & 0 & -\frac{K_f}{M_v} & 0 & -\frac{A_p}{M_v} \\ 0 & 0 & 0 & 0 & 0 & -\frac{4\beta_e A_p}{V_a} - \frac{4\beta_e K_{ca}}{V} \end{bmatrix} \begin{bmatrix} X_1 \\ X_2 \\ X_3 \\ X_4 \\ X_5 \\ X_6 \end{bmatrix} + \begin{bmatrix} 0 & 0 & 0 & 0 & 0 & 0 \\ 0 & 0 & \frac{-1}{M_l} & 0 & 0 & 0 \\ 0 & 0 & 0 & 0 & 0 & \frac{4\beta_e K_{ga}}{V_a} \end{bmatrix} \begin{bmatrix} U_1 \\ U_2 \end{bmatrix}$$

Figure 5. System Equations (Matrix Notation).

## V. ANALYSIS OF SYSTEM PERFORMANCE

Manufacturer's data was consulted in order to formulate a power piston velocity specification. The maximum power piston velocity required was a value of 0.5 in/sec. Common operational velocities ranged between 0.4 - 0.5 in/sec.

### A. PROCEDURE

#### 1. Inputs

Electro hydraulic servovalves have strokes ranging from 0.005 - 0.010 in. for small valves up to 10 gpm capacity to 0.015 to 0.030 in. for 50 gpm valves. In this case, a 15 gpm valve was used and input,  $X_{va}$ , was set from 0.005 to 0.012 in.

An external loading,  $F_l$ , was assumed to range from 0.0 to 40,000. lbf in the simulations. This range of loading could be expected in operational conditions.

#### 2. Outputs

The scheduling of control parameters is shown in Figure 6. Y and X signified the displacement of the power piston and the input piston valve rod assembly.  $P_m$  was the load pressure at the power piston, and  $K_f$  was the fluid spring force at the power piston.

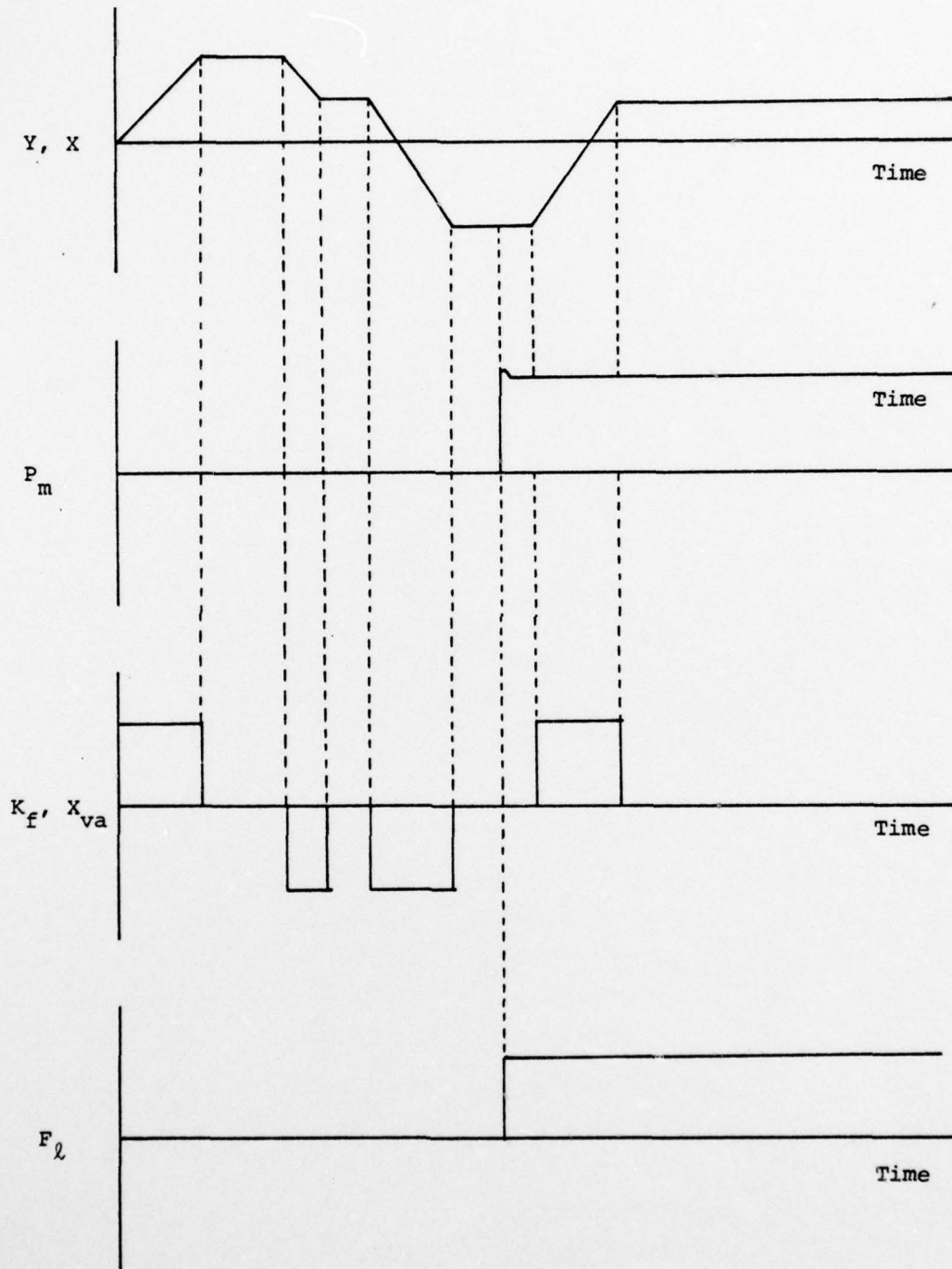


Figure 6. Scheduling of Control Parameters.

## B. COMPUTER SIMULATION RESULT

As mentioned previously, computer simulation results were taken for valve stroke displacements,  $X_{va}$ , from 0.005 to 0.012 in. Figure 7 shows the resulting power piston displacement. As can be seen, the system response is good.

Figure 8 portrays the velocity of the power piston. These data demonstrate that the velocity of the power piston is directly proportional to the displacement of the valve input,  $X_{va}$ . The natural hydraulic frequency of the system was approximately 95 Hz for the control unit input servovalve and piston and 110 Hz for the power piston assembly. These calculations are shown in Appendix B.

Figure 9 is a plot of the load pressure,  $P_m$ , for various external loads. Without external loading,  $P_m$  was almost zero. After an added external load,  $P_m$  was changed slightly for a range of  $F_l$  values from 2000.0 to 40,000.0 lbf.

Calculations show that the displacement of the power piston upon loading is 0.0016 in. for 40,000.0 lbf. Compared to the maximum movement (10.0 in.), this difference is about 0.016 percent. Thus, the displacement of the power piston was almost independent of external loading.

The bulk modulus is a fluid parameter which characterizes the compressibility of the liquid. As can be seen from Figure 10, the value of the bulk modulus has a slight effect on power piston response time. Between bulk modulus values of 100,000 and 300,000 PSI, the power piston response was changed from 0.56 to 0.34 sec. Compared to a maximum required time of 19 to 20 sec, during which the power piston moved 10.0 in., this difference in power piston response time is very

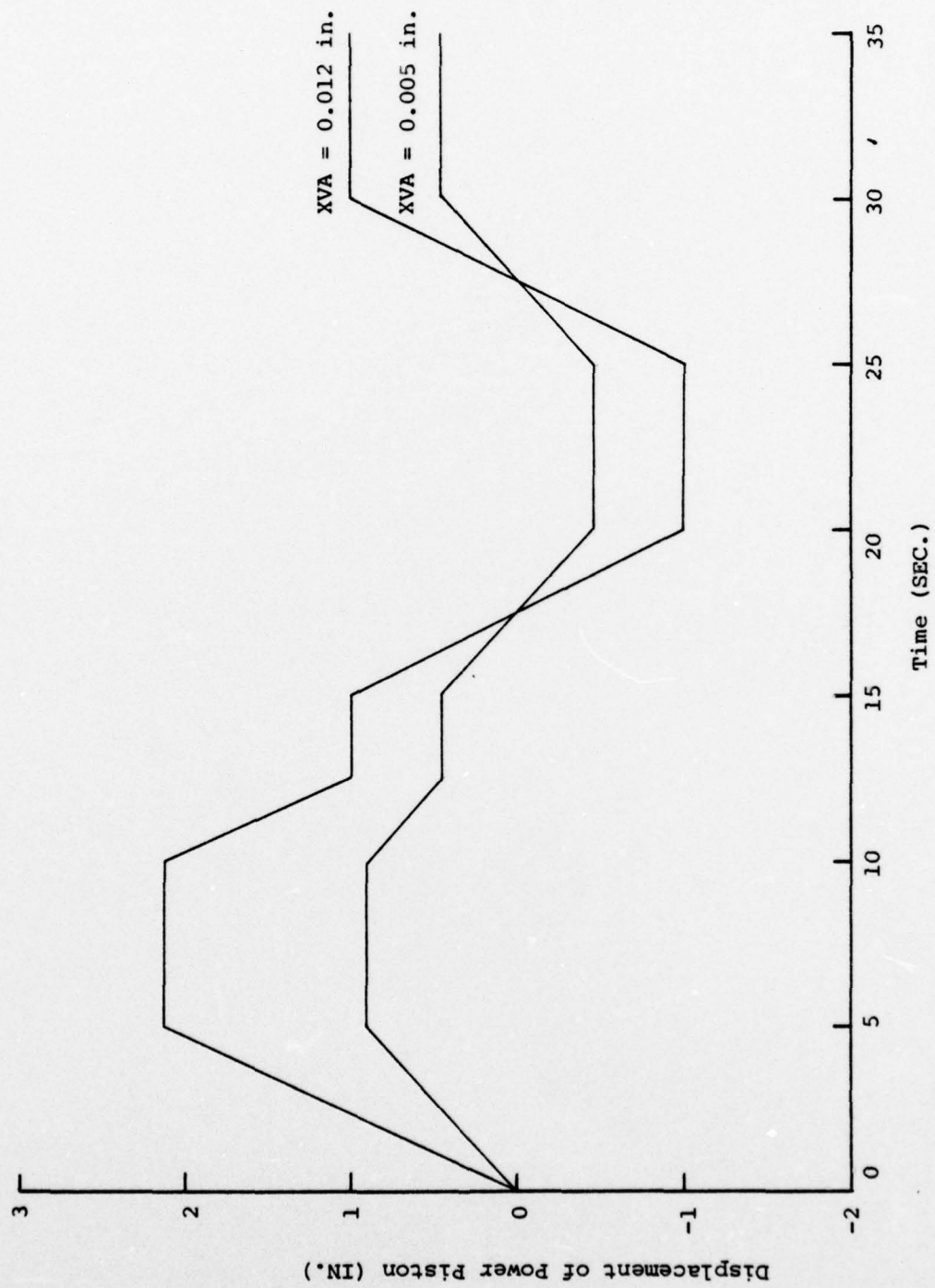


Figure 7. Displacement Response of Power Piston.

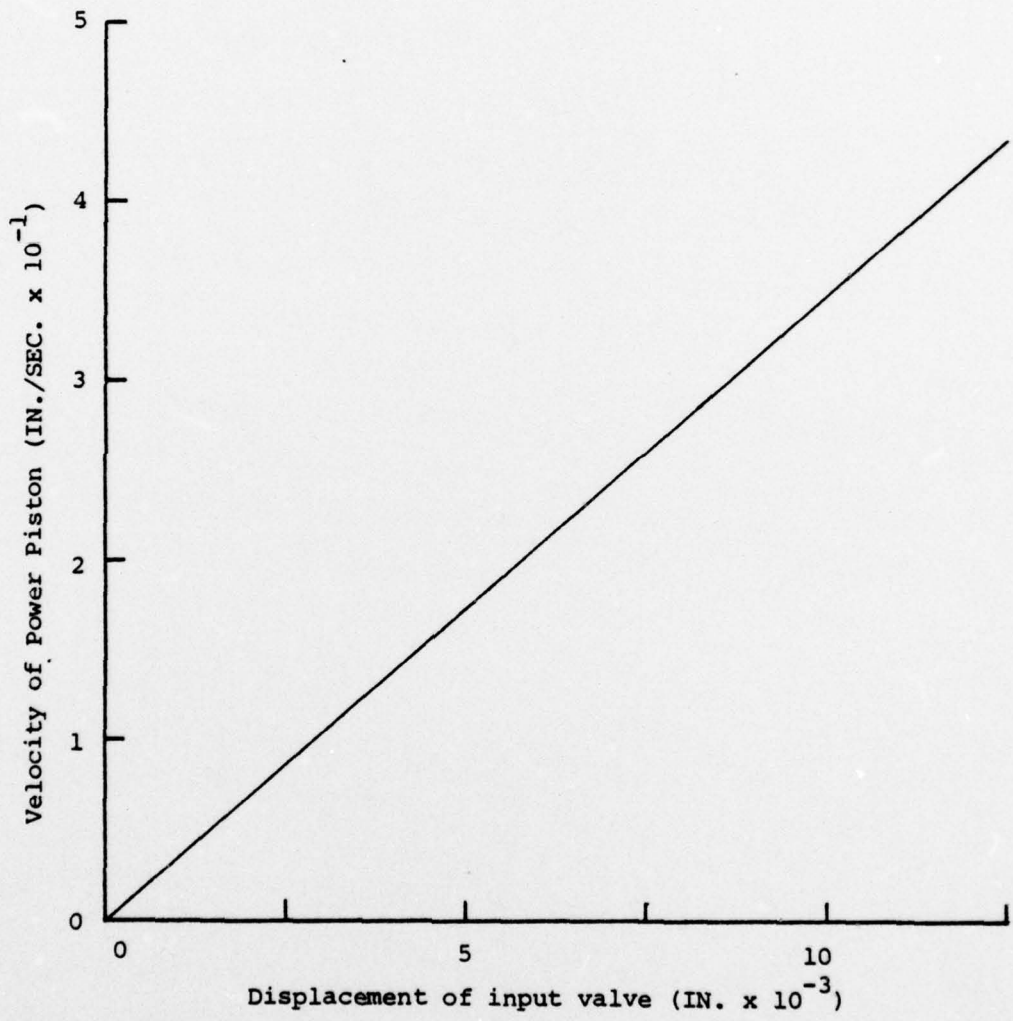


Figure 8. Steady State Velocity Response of Power Piston.



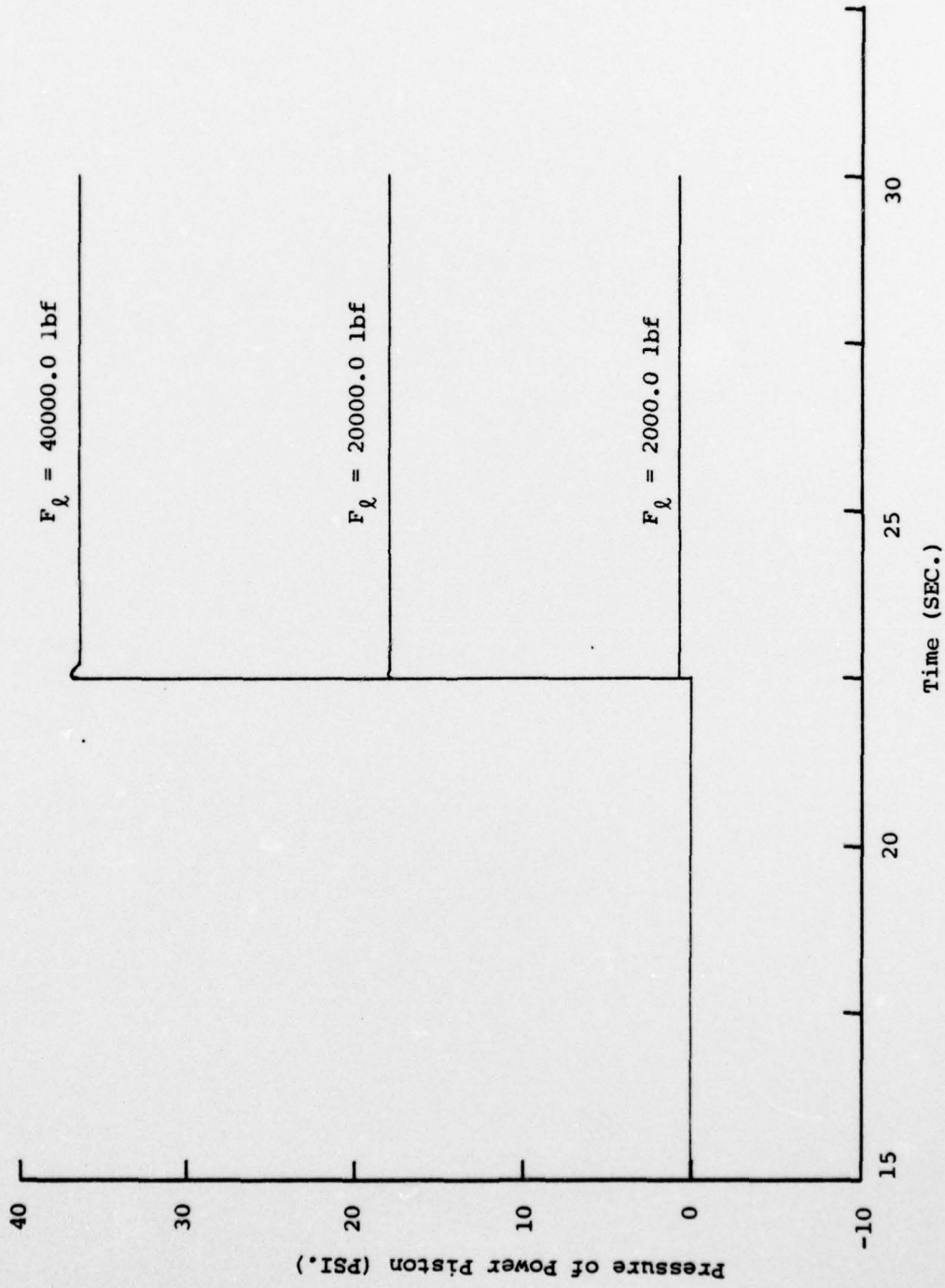


Figure 9. Pressure Response of Power Piston.

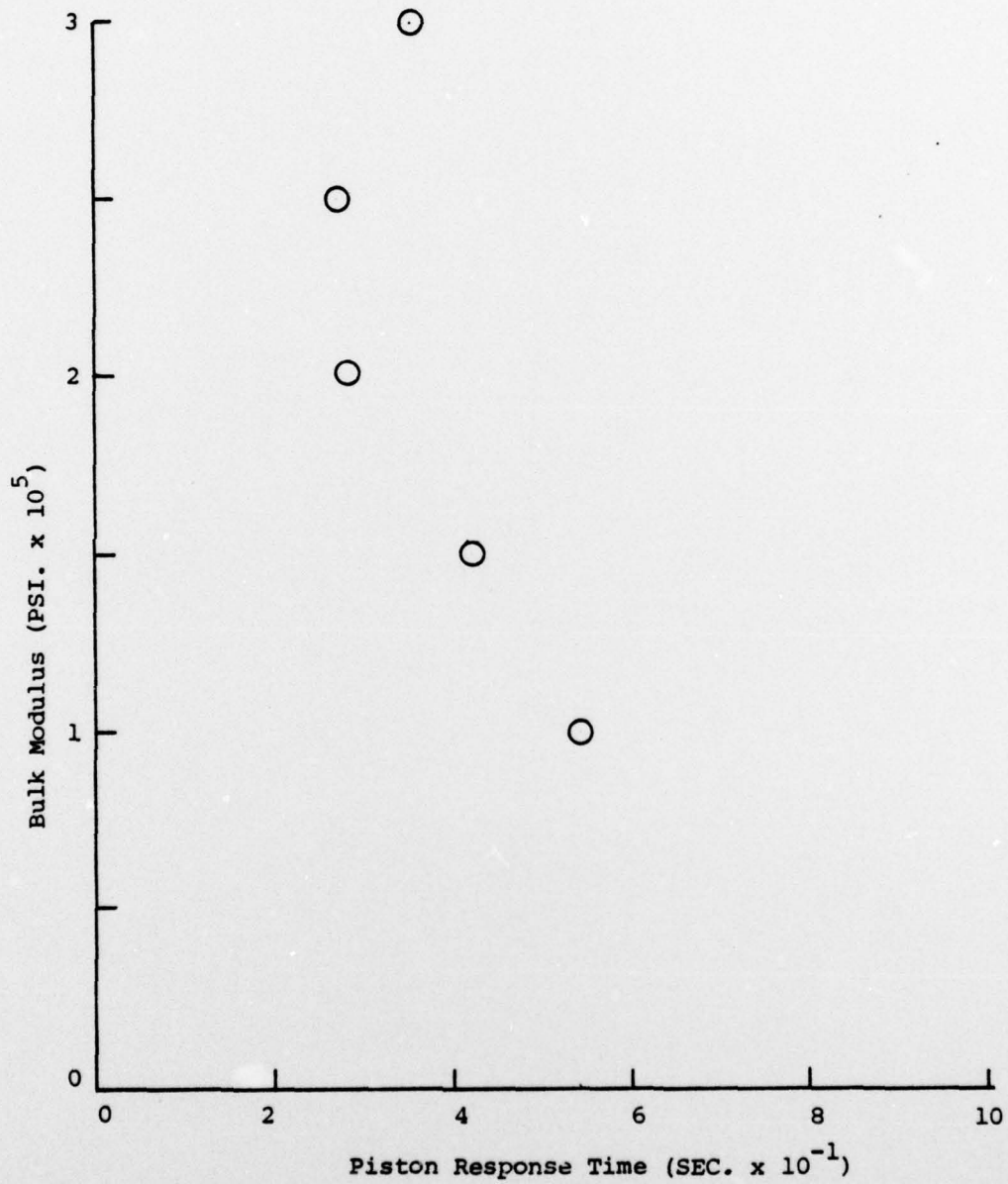


Figure 10. Bulk Modulus Effects on Response.

small. This is an encouraging result since minimizing entrapped gas to insure high  $\beta_e$  values is a difficult and costly process.

Figure 11 shows the influence of bulk modulus on power piston velocity response. Again, in view of a total system response time requirement of 19 to 20 sec, the initial oscillations that occur within the first 0.3 to 0.6 sec of system operation can be considered negligible.

Finally, in Appendix C is shown the computer program developed in this study and a typical computer output (Figure 15).

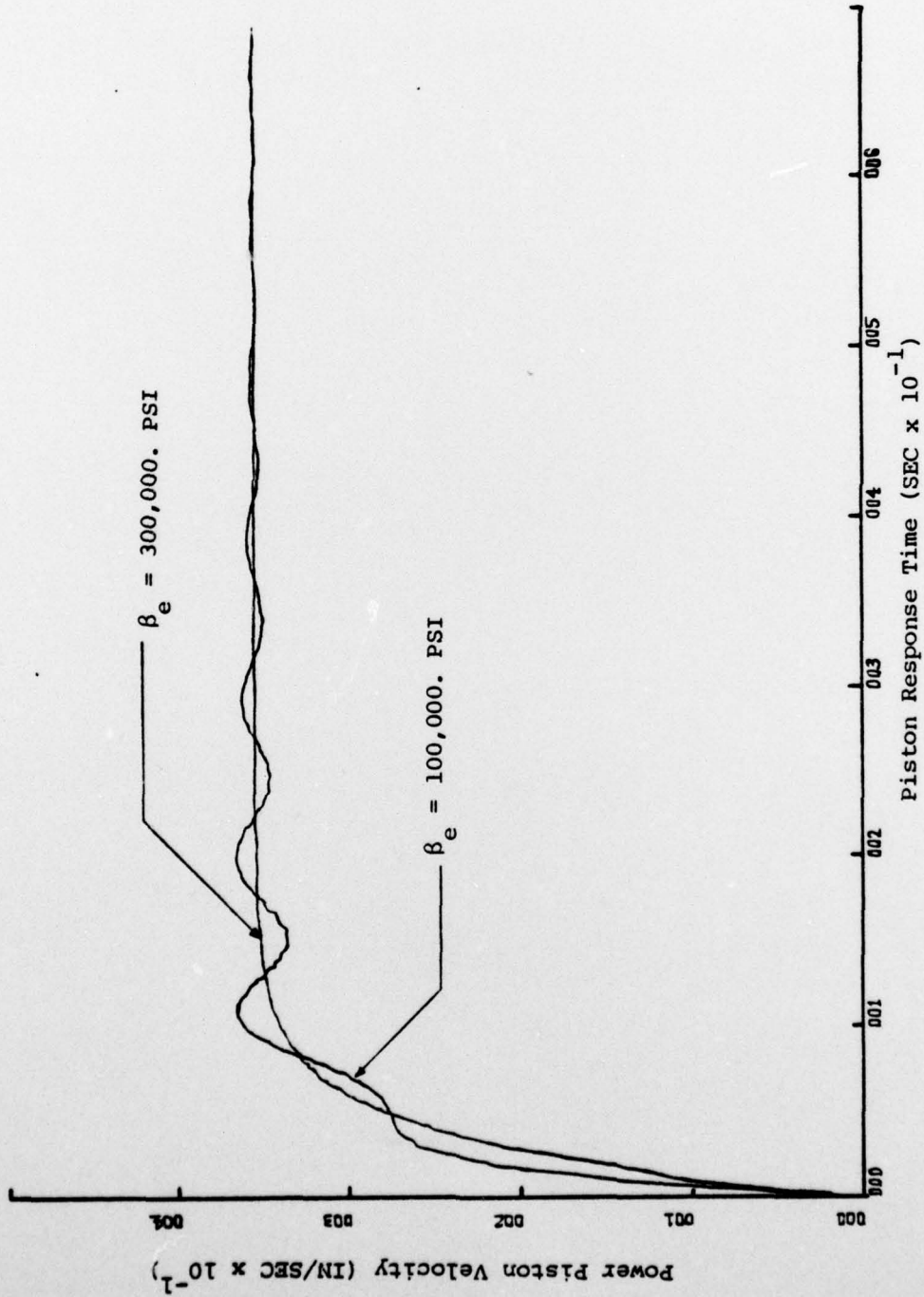


Figure 11. Initial Velocity Response of Power Piston.

## VI. CONCLUSIONS

In this study, several types of C.R.P. systems were analyzed. These included:

1. THE TWO VALVE-PISTON COMBINATION TYPE WITH SOLID CONNECTING ROD  
Results for this system have been presented in the previous sections of this report.
2. A TWO VALVE-PISTON COMBINATION TYPE WITH CONNECTING FLUID LINE OF
  - a. circular pipe construction
  - b. annular pipe construction
  - c. double annular pipe construction

In all of the studies involving fluid lines, the fluid lines had very high frequency and very low damping ratio characteristics. Thus, essentially the influence of the connecting lines on response could be neglected. Appendix D shows the result of various pipe line response calculations.

Computer simulation proved to be a useful design tool regarding the C.R.P. system. Full scale prototype testing, however, is the only conclusive method of proving C.R.P. system response. Unfortunately, testing is both costly and time consuming. Thus, the computer simulation developed in this study could be used to designate critical testing instances and to identify those areas where design efforts would be most productive. In this way, the time involved in optimizing system performance as well as subsequent production costs could be reduced. Likewise, the present computer simulation could be useful in specifying the correct approach for design testing practices.

APPENDIX A: SYSTEM SIGNAL FLOW GRAPH

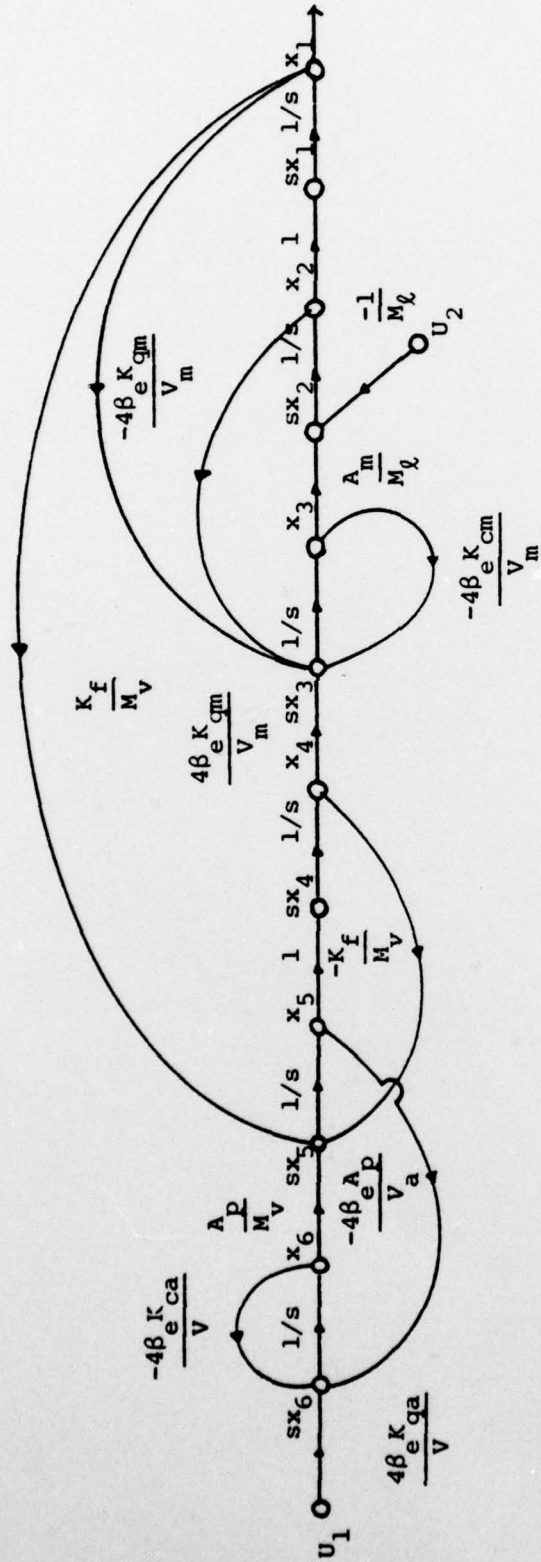


Figure 12. System Signal Flow Graph.

APPENDIX B: SYSTEM RESPONSE

The governing equations could be separated into two parts - the input part (servovalve and piston) and the output part (power piston). In this Appendix, the hydraulic damping coefficient,  $\zeta$ , and the natural frequency,  $\omega_h$ , of each part are determined.

A. INPUT PART (SERVOVALVE AND PISTON)

From the Figure 13, the characteristic equation is

$$C.E = s^2 + \left(\frac{4\beta_e K_{ca}}{V_a}\right) s + \left(\frac{4\beta_e A_p^2}{M_v V_a}\right)$$

$$= s^2 + 2\zeta \omega_h s + \omega_h^2$$

where

$$\omega_h = \sqrt{\frac{4\beta_e A_p^2}{M_v V_a}}$$

$$\zeta = \frac{K_{ca}}{A_p} \sqrt{\frac{\beta_e M_v}{V_a}}$$

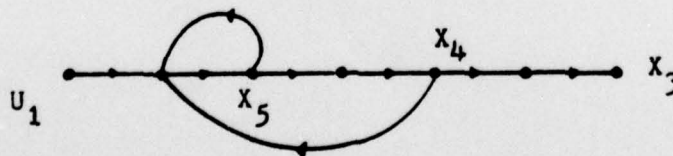


Figure 13. Signal Flow Graph of Input Parts.

For nominal values of bulk modulus, the following results pertain:

$\beta_e$ (PSI)	$\omega_h$ (Hz)	$\zeta$
100,000	95.77	0.00488
300,000	159.83	0.00845

B. OUTPUT PART (POWER PISTON)

From the Figure 14, the characteristic equation is

$$\begin{aligned}
 \text{C.E} &= S^3 + \left(\frac{4\beta_e K_{cm}}{V_m}\right) S^2 + \left(\frac{4\beta_e A^2}{M_\ell V_m}\right) S + \left(\frac{4\beta_e K_{qm} A}{V_m M_\ell}\right) \\
 &= (S + R) (S^2 + 2\zeta \omega_h S + \omega_h^2)
 \end{aligned}$$

Again, for nominal values of bulk modulus, the following results were determined:

$\beta_e$ (PSI)	$\omega_h$ (Hz)	$\zeta$
100,000	110.45	0.00897
300,000	191.29	0.04094

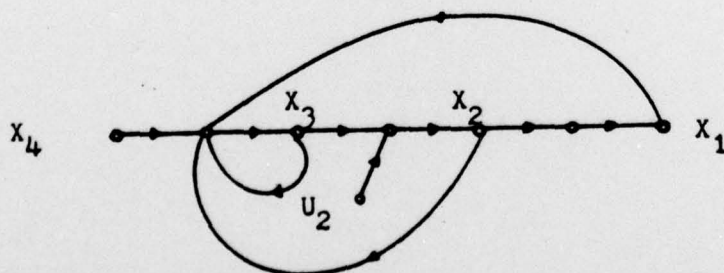


Figure 14. Signal Flow Graph of Output Parts.



APPENDIX C: COMPUTER PROGRAM

```

INITIAL
CONSTANT BE=100000.0
CONSTANT FF=2000.0
CONSTANT CEM=1.54
CONSTANT QMK=33426.54
CONSTANT QAK=2057.08
CONSTANT XM=69.8757
CONSTANT VM=4.9
CONSTANT VA=749.71
CONSTANT VC=14326.0
CONSTANT AM=1102.0
CONSTANT AA=57.67
CONSTANT W=11.938
CONSTANT PS=400.0
CONSTANT PSA=600.0
CONSTANT T1=0.0,T2=0.0,T3=0.0,T4=0.0,T5=0.0,T6=0.0
DYNAMIC
PARAMETER Z=(0.005,0.01,0.012,0.013)
FC=FF*STEP(22.5)
XIN1=Z*STEP(0.0)
XIN2=Z*STEP(5.0)
XIN3=Z*STEP(10.0)
XIN4=Z*STEP(12.5)
XIN5=Z*STEP(15.0)
XIN6=Z*STEP(20.0)
XIN7=Z*STEP(25.0)
XIN8=Z*STEP(30.0)
XVA=XIN1-XIN2-XIN3+XIN4-XIN5+XIN6+XIN7-XIN8
YDD=(AM/XM)*PM-(1./XM)*FC
YD=INTGRL(T1,YDD)
Y=INTGRL(T2,YD)
PMD=-(4.*BE*QMK/VC)*Y-(4.*BE*AM/VC)*YD-(4.*BE*CEM/VC)*PM ...
+(4.*BE*QMK/VC)*X
PM=INTGRL(T3,PMD)
FK=0.86*W*(PS-PM)*(X-Y)
XDD=(FK/VM)*Y-(FK/VM)*X+(AA/VM)*PLA
XD=INTGRL(T4,XDD)
X=INTGRL(T5,XD)
PLAD=-(4.*BE*AA/VA)*XD-(4.*BE*CEA/VA)*PLA+(4.*BE*QAK/VA)*XVA
PLA=INTGRL(T6,PLAD)
OUTPUT Y
PAGE MERGE
METHOD RKSFX
TIMER FINTIM=35.0,OUTDEL=0.5,PRDEL=0.5,DELT=0.002
END
STOP

```

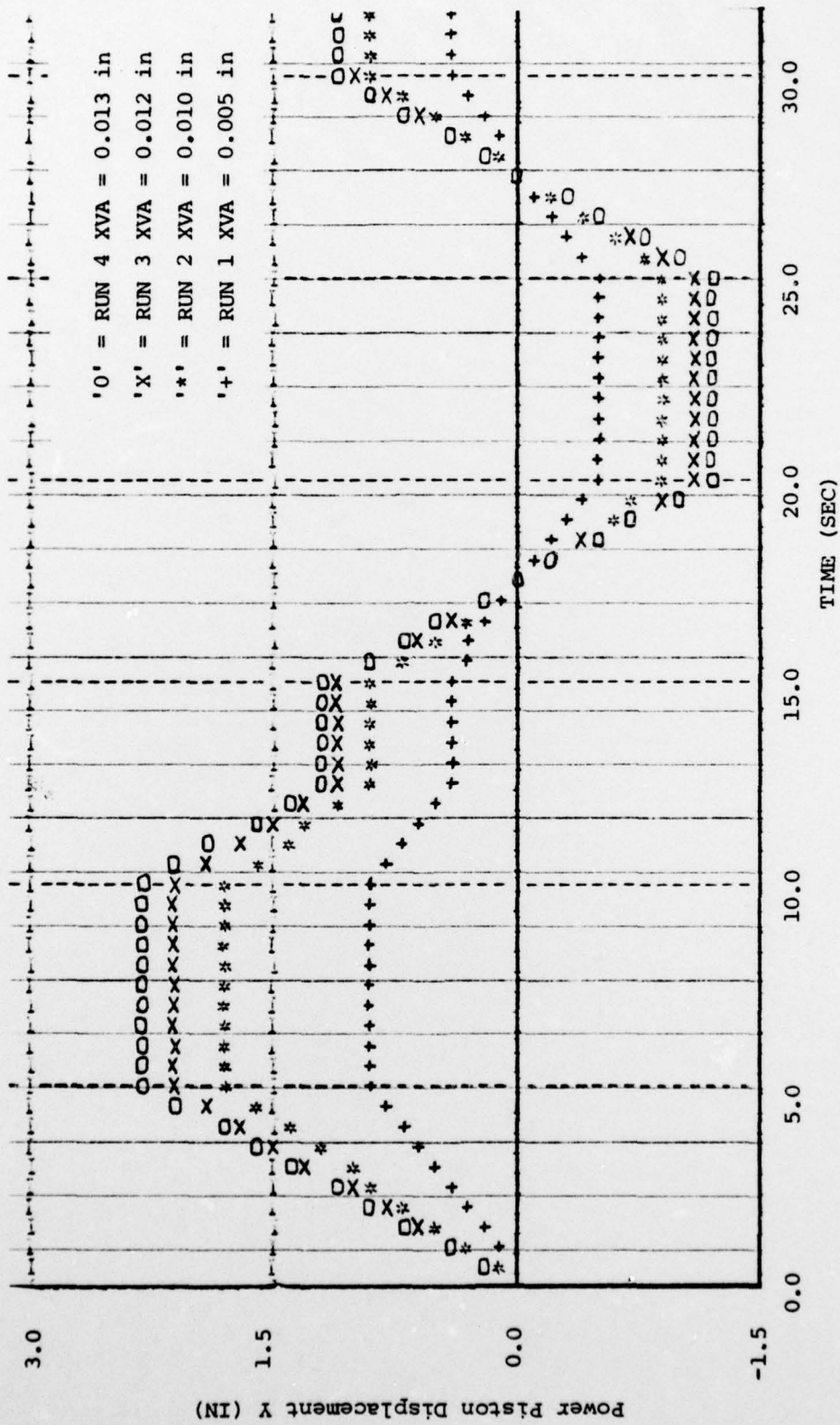
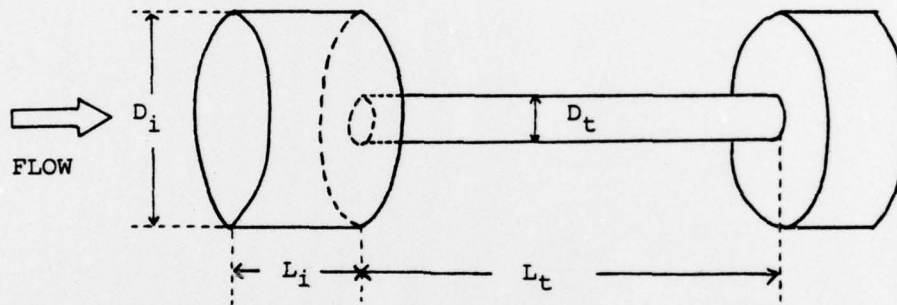


Figure 15. Computer Program Output

APPENDIX D: FLUID LINE RESPONSE

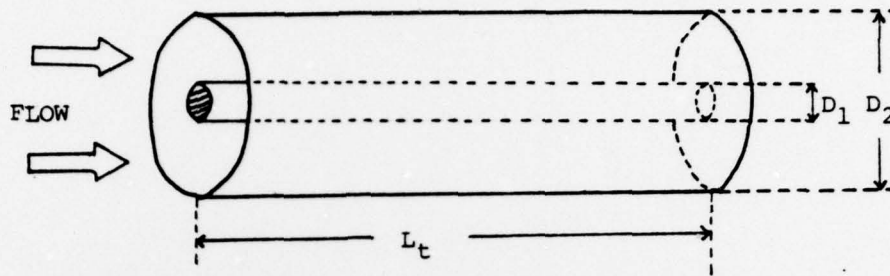
When a fluid is used for transmitting pressure variations, it is necessary to determine the response of the transmission system. In the course of this study, the following line response determinations were formulated.



$$\omega_h = \sqrt{\frac{A_i \beta_e}{\rho(L_i + L_t) v}}$$

$$\zeta = \frac{32\mu L_t}{D_i D_t^2} \sqrt{\frac{v}{\beta_e \rho \pi (L_i + L_t)}}$$

Figure 16. Circular Type of Line Response Determinations.



$$\omega_h = \sqrt{\frac{\beta_e A_i}{\rho(L_i + L_t)v}}$$

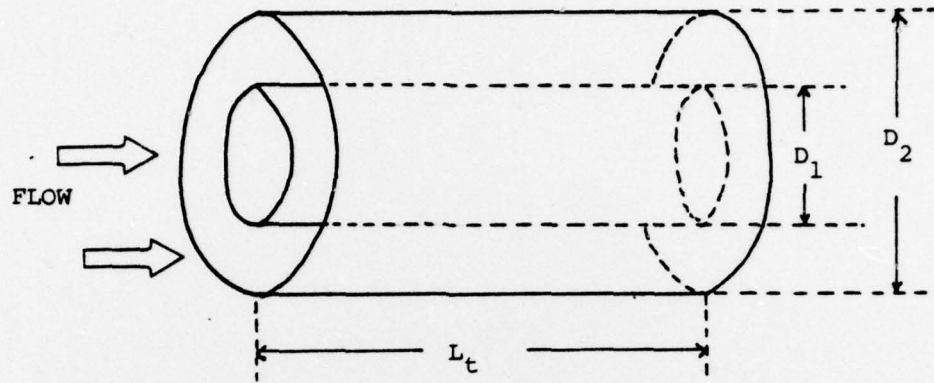
$$\zeta = \frac{32\mu L_t (K_2 D_2 + K_1 D_1)}{D_i^2 D_2^2} \sqrt{\frac{v}{\rho\pi\beta_e (L_i + L_t)}}$$

$$K_1 = \frac{4r_{\max}^2 - D_1^2}{D_1(D_2 + D_1 - 8r_{\max}^2)}$$

$$K_2 = \frac{D_2^2 - 4r_{\max}^2}{D_2(D_2 + D_1 - 8r_{\max}^2)}$$

$$r_{\max} = \sqrt{\frac{(D_2/2)^2 - (D_1/2)^2}{2\ln(D_2/D_1)}}$$

Figure 17. Annular Type of Line Response Determinations.



$$\omega_h = \sqrt{\frac{\beta_e A_i}{\rho(L_i + L_t)v}}$$

$$\zeta = \frac{32\mu L_t (1 + K_1 D_1 + K_2 D_2)}{D_i D_2^2} \sqrt{\frac{v}{\rho\pi\beta_e (L_i + L_t)}}$$

Figure 18. Double Annular Type of Line Response Determinations.

LIST OF REFERENCES

1. Wind, J., "Principles of Mechanisms in C.R.P. Systems," Int'l Shipbuilding Prog., No. 198, Pg. 80-94, Feb. 1971.
2. Ogata, K., Modern Control Engineering, Prentice-Hall, New York, 1970.
3. Merritt, H. E., Hydraulic Control Systems, John Wiley and Sons, New York, 1967.
4. Blackburn, J. F., Reethof, G., and Shearer, J. L., Fluid Power Control, John Wiley and Sons, New York, 1960.
5. C. R. P. System Engineering Drawings, Bird-Johnson Co., Walpole, Mass., 1977.
6. Ward, J. R., and Strum, R. D., State Variable Analysis, Prentice-Hall, New York, 1970.

INITIAL DISTRIBUTION LIST

	No. Copies
1. Defense Documentation Center Cameron Station Alexandria, Virginia 22314	2
2. Library, Code 0142 Naval Postgraduate School Monterey, California 93940	2
3. Department Chairman, Code 69Fu Department of Mechanical Engineering Naval Postgraduate School Monterey, California 93940	2
4. Associate Professor Thomas M. Houlihan, Code 69Hm Department of Mechanical Engineering Naval Postgraduate School Monterey, California 93940	5
5. Curricular Officer, Code 34 Department of Mechanical Engineering Naval Postgraduate School Monterey, California 93940	1
6. Lt. Masaaki Kanazawa Ship Engineering Section Technical Division, MSO 9 - 7 - 45 Akasaka, Minatoku Tokyo, Japan 107	2
7. Associate Professor Robert H. Nunn, Code 69Nn Department of Mechanical Engineering Naval Postgraduate School Monterey, California 93940	1